

The Influence of Thermal Annealing on Texture of Yttrium Stabilized Zirconia Thin Films

Giedrius LAUKAITIS^{1*}, Oresta LIUKPETRYTĖ¹, Julius DUDONIS¹, Darius MILČIUS²

¹Physics Department, Kaunas University of Technology, Studentų 50, LT-51368 Kaunas, Lithuania

²Lithuania Energy Institute, Breslaujos 3, LT-44403 Kaunas, Lithuania

Received 06 September 2007; accepted 09 October 2007

Yttrium stabilized zirconia (YSZ) thin films were grown evaporating tetragonal phase zirconia stabilized by 8 wt. % of yttrium (8YSZ) ceramic powder. YSZ thin films were deposited on optical quartz substrates using e-beam deposition technique controlling deposition parameters: substrate temperature and electron gun power influencing thin film properties. YSZ thin films (1.5 μm – 2 μm of thickness) were deposited at different substrate temperatures (250 °C, 400 °C, 600 °C) and the electron gun power was 0.66 kW, 0.9 kW, 1.05 kW, and 1.2 kW during thin films deposition. To understand the stability and influence of temperature on the structure of formed thin films the deposited YSZ layers were annealed at 1100 °C temperature, in air and were investigated by X-ray diffraction (XRD). It was found that annealing temperature, electron gun power, and substrate temperature influence the crystallite size of YSZ: crystallite size before annealing was 12.2 nm – 46.2 nm and after annealing was 23 nm – 49.8 nm. It was found that the main orientation of the YSZ thin films texture repeats the characteristics of the evaporated YSZ powder and dominant crystal structure of tetragonal phase of YSZ thin films is (101). The same (101) tetragonal phase remains after annealing at 1100 °C temperature. The crystallite size and coefficient of texture increases but repeats the character of the curves as it was before the annealing. The temperature and substrate material does not influence the texture of YSZ thin films.

Keywords: YSZ thin films, electron beam deposition, thermal treatment.

INTRODUCTION

The widespread commercialization of the solid oxide fuel cells (SOFC) will depend greatly on lowering material costs and achieving even greater gains in efficiency [1 – 3]. SOFC differ in many respects from the other fuel cells technology: they are composed of all-solid-state materials, the cells can operate at temperature as high as 1000 °C, significantly hotter than any other major category of the fuel cells. Electrolyte has the biggest influence for the SOFC performance. Different types of electrolyte materials could be used such as lanthanum gallate ceramic including lanthanum strontium gallium magnesium, bismuth yttrium oxide, barium cerate, strontium cerate, zirconium oxide or cerium oxide stabilized by rare earth oxides and etc. [1 – 7].

For stabilizing ZrO₂ could be used dopants such as CaO, MgO, Sc₂O₃ and certain rare earth oxides such as Nd₂O₃, Sm₂O₃, Yb₂O₃. Zirconia based mixed conductors have many applications such as: electrodes, membranes for gas separation, and electrocatalytic reactors [8]. These materials can be used as gas separator for the decomposition of water vapor into hydrogen and oxygen at high temperature as they are considered to be heat resistant and mechanically stable [9].

Yttrium - stabilized zirconium oxide – (ZrO₂)_{0.92}(Y₂O₃)_{0.08} – YSZ cermets is very interesting material because of high chemical stability, electrical resistivity, magnetic permittivity, low thermal conductivity, etc.

YSZ is the most widely adopted and popular material for SOFC electrolytes because it conducts only oxygen ions over a wide range of oxygen partial pressures. It is

conditioned by low YSZ electrolyte price, good thermal properties (caused by high operating temperature), and ionic conductivity. SOFCs based on bulk (200 μm – 500 μm thick) YSZ membranes are normally operated at temperatures above 800 °C to achieve sufficiently high oxygen ion conductivity. Today it is widely accepted that lowering the operating temperature of SOFCs in the range of 600 °C – 700 °C is preferable for several reasons: lowering of the operating temperature of SOFC can provide higher thermodynamic efficiency, higher Nernstian voltages, enhanced durability of cell performance, and the usage of cheaper stainless steel interconnects and compliant temperature gaskets [10]. One of the ways for lowering the cost and increasing the performance of SOFC is to use as much as possible thinner electrolyte layers (that is lowering the working temperature of the SOFC and the costs of the other components of fuel cell – FC). Moreover, the electrolyte should be made not porous on the porous substrates [11]. The shortcut between anode and cathode is the second problem. That has the influence on the electrolyte thickness (by now it is 2 μm – 3 μm of range).

The problem can be solved using YSZ thin films. The variety of chemical and physical methods, such as metal organic chemical vapor deposition (MOCVD), chemical vapor deposition (CVD), spray pyrolysis, physical vapor deposition (PVD) and etc. for producing solid oxide electrolyte thin films exist [12 – 19]. PVD could be one of the best techniques for getting good quality YSZ thin films. It is easier to control thin film properties using PVD technology, compare to other technique [20].

In the present study, YSZ electrolyte thin films were deposited using e-beam deposition technique on optical quartz substrates. Tetragonal phase YSZ powder was used. The formed YSZ thin films were thermally annealed at

*Corresponding author. Tel.: +370-37-300349; fax: +370-37-456472.
E-mail address: gielauk@ktu.lt (G. Laukaitis)

1100 °C temperature in the air atmosphere. That was done to study the stability of formed YSZ thin films and to understand the influence of annealing temperature and technological parameters on YSZ thin films texture, crystallite size, and homogeneity.

EXPERIMENTAL

YSZ thin films were deposited by e-beam deposition technique (OIHO – 7 – 004 PVD system) from tetragonal phase ZrO₂ stabilized by 8 mol% of Y₂O₃ (8YSZ) ceramic powder (SIGMA-ALDRICH submicron powder, 99.9 % purity based on trace metal analysis, 1.68 μm micron average particle size). Before deposition YSZ powder was pressed to the pellets of 25 mm diameter and 2 mm of thickness. YSZ thin films (1.5 μm – 2 μm of thicknesses) were deposited on optical quartz (SiO₂) at different substrate temperatures and e-beam power (deposition rates). The samples were cleaned in the ultrasonic bath (acetone solution) before deposition. More details on the technical parameters and experimental equipment of the used technique are presented in [20]. Residual gas pressure in the vacuum chamber was 4×10^{-3} Pa. The distance between electron gun and substrate was fixed at 240 mm. The substrate was additionally heated by a heater to temperatures from 20 °C to 600 °C (with error of 5 °C). The deposition rate was evaluated from the thin film final thickness measurements.

The film structure was analyzed by X-ray diffraction (XRD) (DRON – UM1 with standard Bragg-Brentano focusing geometry with a error of 0.01°) in a 10° – 80° range using the Cu K_α ($\lambda = 0.154059$ nm) radiation. The crystallite size d of YSZ thin films was estimated from the Scherrer's equation and using XFIT program with Voigt function modeling [22 – 23].

The XRD results were quantified by defining a simple texture coefficient R [24] which is the ratio of the intensities of the (101) peak to the sum of the intensities of all peaks. As the spectra consisted of (101), (110), (200), (211), (202) peaks, the coefficient becomes:

$$R_{101} = I_{101} / (I_{101} + I_{110} + I_{200} + I_{211} + I_{202}). \quad (1)$$

The value $R = 0.57$ corresponds the random orientation, and $R = 1$ means preferred (101) orientation.

The formed YSZ thin films were thermal annealed in the laboratory furnace at 1100 °C temperature in the air. A Scanning Electron Microscope (SEM, JSM5600) with assembled EDS (Energy Dispersive Spectrometer) was used to investigate the concentration of elements in the formed YSZ thin films.

RESULTS AND DISCUSSIONS

The XRD diffraction patterns of the pressed YSZ powder were presented in [21]. They show that the positions of the Bragg peaks are typical for the tetragonal 8YSZ (according to Crystallographica Search-Match, Version 2). XRD peaks of YSZ thin films indicate sharp (101) and minor (110), (200), (211) and (202) orientations. These YSZ thin films repeat the crystal structure of the chosen evaporated YSZ material [22]. The sharpness of (101) XRD peaks indicates high degree of homogeneity of the YSZ thin films (Fig. 1).

Three types of materials: crystalline (Alloy 600, Fe-Ni-Cr), polycrystalline (Al₂O₃), and amorphous (optical quartz, SiO₂) substrates were chosen in order to understand the influence of substrate material on the crystal orientation of deposited YSZ thin film using e-beam deposition technique in the [20] work. It was found that the substrate has no influence on the crystal structure of the YSZ thin film. For that reason only one type substrate – optical quartz (SiO₂) was chosen in this work. To understand e-beam gun power influence on YSZ thin film formation when tetragonal phase YSZ ceramic powder is evaporated, thin films were deposited at different gun powers: 0.75, 0.9, 1.05, and 1.2 kW.

To get denser thin film and control the crystallite size influencing the ionic conductivity of formed layers it is possible by changing the substrate temperature during the deposition.

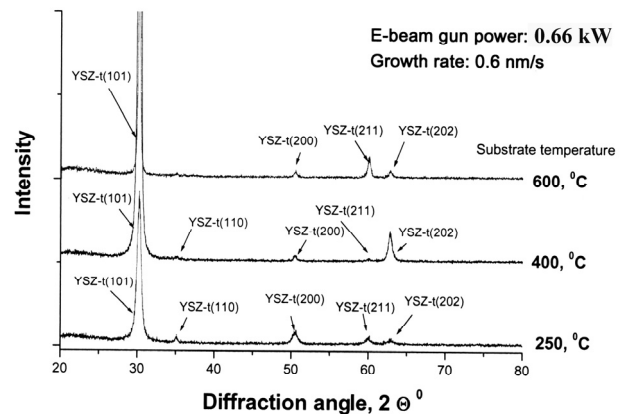


Fig. 1. XRD patterns of YSZ thin films deposited on SiO₂ substrates at 0.66 kW e-beam gun power (substrate temperatures are 250 °C, 400 °C, 600 °C)

It was found that the substrate temperature (from 200 °C to 600 °C) has no influence on the crystal orientation of the YSZ thin film (Fig. 1) at low e-beam gun powers (<0.9 kW) and thin film deposition rates (<1.5 nm/s) [21]. Similar results were received using CVD technique [25]. XRD measurements start to show cubic ZrO₂ peaks when e-beam gun power is higher than 1.0 kW (deposition rate >1.5 nm/s) [21]. The thin films start to have two different phases: tetragonal YSZ and cubic ZrO₂ at high e-beam gun power. From that it is possible to conclude that the YSZ material at the high e-beam gun power from the evaporant start to evaporate in the different types of clusters.

The results show that the substrate temperature and e-beam gun power has the influence on the crystallite size of the YSZ thin film. The crystallite size is increased from 120 nm to 230 nm by changing the e-beam gun power at 250 °C substrate temperature (Table 1). The crystallite size is decreased from 250 nm to 140 nm by increasing gun power at 400 °C substrate temperature and keeping the same at 600 °C substrate temperature.

Substrate temperature and e-beam gun power has an influence on the crystallite size of the YSZ thin film. The lowest crystallite size (12 nm) was found when $P = 0.66$ kW and $T_s = 250$ °C; the biggest (46 nm) – $P = 0.9$ kW and $T_s = 400$ °C (Table 1). Crystallite size increases linearly

from 12.2 nm to 29.4 nm at 0.66 kW e-beam gun power at the higher temperature (250 °C – 600 °C) also. The crystallite size decreases and has minimum values (decreasing up to 13.4 nm) at 400 °C substrate temperature

when e-beam gun power is higher than 0.66 kW. It could cause that at lower temperatures, because of lower atom mobility, the time for adatom to find adsorption site exceeds the relaxation time.

Table 1. YSZ thin film crystallites size d (extracted from XRD data) dependence on substrates temperature T_s (250 °C, 400 °C and 600 °C) at different e-beam gun powers P (0.66 kW, 0.9 kW, 1.05 kW and 1.2 kW) and annealed at 1100 °C temperature in air atmosphere

P , kW	T_s , °C	250		400		600	
		d_1 , nm	d_2 , nm	d_1 , nm	d_2 , nm	d_1 , nm	d_2 , nm
0.66		12.2	31.0	25.6	37.7	29.8	40.5
0.90		27.3	34.1	46.2	49.8	32.6	34.9
1.05		13.8	29.8	13.4	28.9	30.1	40.9
1.20		17.9	33.9	15.8	23.0	22.3	28.7

d_1 – crystallite size before heat treatment, d_2 – crystallite size after heat treatment.

Table 2. Dependence of YSZ thin films texture coefficients R (normalized to different peaks intensities) on the electron gun power at different substrate temperatures before thermal annealing

E-beam gun power, kW	Substrate temperature, °C	R_1	R_2	R_3	R_4	R_5
		101/(101+110+200+211+202)	101/(101+110)	101/(101+200)	101/(101+211)	101/(101+202)
YSZ initial material		0.588	0.880	0.739	0.856	0.957
0.66	250	0.784	0.932	0.917	0.949	0.945
0.90		0.946	0.990	0.99	0.995	0.969
1.05		0.511	0.604	0.945	0.842	0.947
1.20		0.597	0.836	0.931	0.9	0.915
0.66	400	0.956	0.995	0.994	0.995	0.972
0.90		0.615	0.755	0.988	0.798	0.966
1.05		0.774	0.949	0.963	0.889	0.930
1.20		0.407	0.480	0.922	0.851	0.894
0.66	600	0.868	0.977	0.969	0.94	0.968
0.90		0.956	0.997	0.994	0.991	0.973
1.05		0.972	0.998	0.998	0.996	0.980
1.20		0.327	0.443	0.831	0.667	0.913

Table 3. Dependence of YSZ thin films texture coefficients R (normalized to different XRD peaks intensities) on the electron gun power at different substrate temperatures after thermal annealing at 1100 °C

E-beam gun power, kW	Substrate temperature, °C	R_1	R_2	R_3	R_4	R_5
		101/(101+110+200+211+202)	101/(101+110)	101/(101+200)	101/(101+211)	101/(101+202)
0.66	250	0.801	0.942	0.922	0.942	0.962
0.90		0.953	0.991	0.993	0.994	0.974
1.05		0.463	0.554	0.952	0.803	0.943
1.20		0.987	0.995	0.999	0.996	0.997
0.66	400	0.962	0.995	0.995	0.996	0.976
0.90		0.612	0.770	0.983	0.777	0.970
1.05		0.875	0.981	0.980	0.940	0.962
1.20		0.569	0.647	0.968	0.886	0.953
0.66	600	0.848	0.984	0.968	0.913	0.967
0.90		0.953	0.997	0.995	0.986	0.974
1.05		0.967	1.000	0.997	0.993	0.976
1.20		0.437	0.571	0.881	0.754	0.928

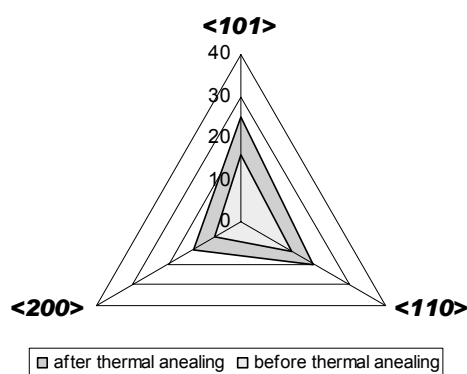


Fig. 2. YSZ thin film crystallite size d (extracted from XRD data) at different crystallographic orientation before and after thermal annealing at 1100 °C temperature in air (at 1.05 kW e-beam gun power and 400 °C substrates temperature)

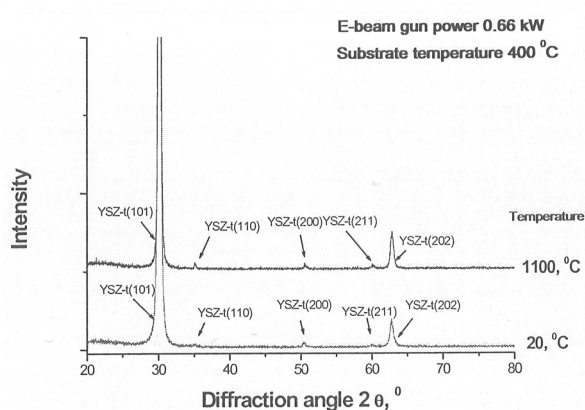


Fig. 3. XRD patterns of YSZ thin films deposited on SiO₂ substrates at 0.66 kW e-beam gun power at 400 °C substrates temperature and annealed at 1100 °C temperature in air

As the atom mobility increases at higher temperatures, this time decreases. As a result, the curve of crystallite size versus temperature passes the minimum and that is more pronounced at higher e-beam powers (higher thin film growth rate).

The texture coefficient as a function of electron gun power at different substrate temperatures during the deposition of YSZ thin films is shown in Tables 2, 3. The films grow with preferred (101) orientation. The texture (101) dominates in the electron gun power interval (0.75 kW – 0.9 kW) when the substrate temperature is 250 °C. The same texture (101) at higher temperatures (400 °C – 600 °C) dominates but it is registered in the wider electron gun power region (0.75 kW – 1.05 kW).

The formed YSZ thin films were thermal annealed in the furnace at 1100 °C temperature in the air atmosphere. That was done to finding out about the stability of formed YSZ thin films and to understand the influence of annealing temperature on crystallite size. It was found that crystallite sizes increases after annealing and that depends on the deposition parameters: T_s substrate temperature and P e-beam gun power (Table 1). The tendency of crystallite size dependence on technological parameters is similar as was before annealing (Table 1), only the crystallite size increases (Fig. 2). The biggest increase was found when

$T_s = 250$ °C. XRD peaks of YSZ thin films indicate that the dominating tetragonal (101) crystallographic orientation is the same (Fig. 3) as was before annealing at 1100 °C temperature and it repeats the crystal structure of the chosen evaporated YSZ material. The texture coefficient increases after the thermal annealing (Tables 2, 3). That shows that the annealing at 1100 °C did not change the crystallites orientation and they only increase in the main crystal orientations as it was before thermal treatment.

EDS measurements show that the formed YSZ thin films are stoichiometric and repeat the stoichiometry of elements of the chosen evaporated YSZ material. The annealing at 1100 °C temperature did not influence the stoichiometry of the formed YSZ thin films.

CONCLUSIONS

The obtained results show that YSZ thin films deposited on the optical quartz (SiO₂) substrates, when evaporating material was tetragonal phase ZrO₂ stabilized by 8 mol % of Y₂O₃ (8YSZ) ceramic powder, are tetragonal with dominating texture (101) and reproduce the crystal structure of the chosen evaporated YSZ material. The texture (101) dominates at lower e-beam gun powers. Also, the XRD measurements show cubic ZrO₂ peaks at higher e-beam gun powers and thin films start to have two different phases: tetragonal YSZ and cubic ZrO₂. So, it is possible to conclude that the YSZ material at high e-beam gun powers starts to evaporate (from the evaporant) in the different types of clusters. That also allows changes in texture. The lowest crystallite size (12.2 nm) was found when e-beam gun power (P) 0.66 kW and substrate temperature (T_s) 250 °C; the biggest (46.2 nm) – $P = 0.9$ kW and $T_s = 400$ °C. The thermal annealing at 1100 °C temperature in air does not change dominating tetragonal (101) crystallographic orientation of YSZ thin films. The crystallite size and texture increase but follows the character of the curves as it was before annealing. The stoichiometry of elements of the formed YSZ thin films corresponds to the evaporated initial material.

Acknowledgement

The work was supported by the Lithuanian State Science and Studies Foundation.

REFERENCES

1. **Boudghene, Stambouli, Traversa, E.** Solid Oxide Fuel Cells (SOFCs): a Review of an Environmentally Clean and Efficient Source of Energy *Renewable and Sustainable Energy Reviews* 6 (5) 2002: pp. 433 – 455.
2. **Tu, H., Stimming, U.** Advances, Aging Mechanisms and Lifetime in Solid-oxide Fuel Cells *Journal of Power Sources* 127 (1 – 2) 2004: pp. 284 – 293.
3. **Tietz, F., Buchkremer, H.-P., Stover, D.** Components Manufacturing for Solid Oxide Fuel Cells *Solid State Ionics* 152–153 2002: pp. 373 – 381.
4. **Masayuki Dokiya.** SOFC System and Technology *Solid State Ionics* 152 – 153 2002: pp. 383 – 392.
5. **Fukushima, Y., Shimada, M., Kraines, S., Hirao, M., Koyama, M.** Scenarios of Solid Oxide Fuel Cell Introduction into Japanese Society *Journal of Power Sources* 131 Issues 1 – 2 2004: pp. 327 – 339.

6. **Minh Nguyen, Q.** Solid Oxide Fuel Cell Technology – Features and Applications *Solid State Ionics* 174 2004: p. 271.
7. **Zhang, T. S., Ma, J., Luo, L. H., Chan, S. H.** Preparation and Properties of Dense $Ce_{0.9}Gd_{0.1}O_{2-\delta}$ Ceramics for Use as Electrolytes in IT-SOFCs *Journal of Alloys and Compounds* 422 2006: pp. 46 – 52.
8. **Iwahara, H., Esaka, T., Takeda, K.** Advances in Ceramics *In: Science and Technology of Zirconia* Vol. 24 American Ceramic Society, Columbus, OH, 1988: p. 907.
9. **Naito, H., Arashi, H.** Hydrogen Production from Direct Water Splitting at High Temperatures Using a ZrO_2 - TiO_2 - Y_2O_3 Membrane *Solid State Ionics* 79 1995: p. 366.
10. **Bohac, P., Orliukas, A., Gauckler, L. J.** Ed. Ulf Bossel. *Proc. 1st European Solid Oxide Fuel Cells Forum*, 3–7 October 1994, Lucerne, Switzerland Vol. 2, 1994: p. 651.
11. **Larminie, J., Dicks, A.** Fuel Cells Systems Explained. John Wiley & Sons Ltd., 2003: 406 p.
12. **Snijkers, F., de Wilde, A., Mullens, S., Luyten, J.** Aqueous Tape Casting of Yttria Stabilised Zirconia Using Natural Product Binder *Journal of the European Ceramic Society* 24 2004: pp. 1107 – 1110.
13. **Wang, H. B., Xia, C. R., Meng, G. Y., Peng, D. K.** Deposition and Characterization of YSZ Thin Films by Aerosol-assisted CVD *Materials Letters* 44 2000: pp. 23 – 28.
14. **Charojrochkul, S., Choy, K. L., Steele, B. C. H.** Flame Assisted Vapour Deposition of Cathode for Solid Oxide Fuel Cells. 1. Microstructure Control from Processing Parameters *Journal of the European Ceramic Society* 24 2004: pp. 2515 – 2526.
15. **Wanzenberg, E., Tietz, F., Kek, D., Panjan, P., Stover, D.** Influence of Electrode Contacts on Conductivity Measurements of Thin YSZ Electrolyte Films and the Impact on Solid Oxide Fuel Cells *Solid State Ionics* 164 2003: pp. 121 – 129.
16. **Horita, S., Nakajima, H., Kuniya, T.** Improvement of the Electrical Properties of Heteroepitaxial Yttria-stabilized Zirconia (YSZ) Films on Si Prepared by Reactive Sputtering *Vacuum* 59 2000: pp. 390 – 396.
17. **Nagata, A., Okayama, H.** Characterization of Solid Oxide Fuel Cell Device Having a Three-layer Film Structure Grown by RF Magnetron Sputtering *Vacuum* 66 2002: pp. 523 – 529.
18. **Caricato, A. P., Di Cristoforo, A., Fernandez, M., Leggieri, G., Luches, A., Majni, G., Martino, M., Mengucci, P.** Pulsed Excimer Laser Ablation Deposition of YSZ and TiN/YSZ Thin Films on Si Substrates *Applied Surface Science* 208 – 209 (1–4) 2003: pp. 615 – 619.
19. **Ju Hyung Suh, Sang Ho Oh, Hyung Seok Kim, Se-Young Choi, C.-G. Chan-Gyung Park.** Effects of Neutralizers on the Crystal Orientation of YSZ Films Grown by Using Ion Beam Sputtering *Vacuum* 74 Issues 3-4 2004: pp. 423 – 430.
20. **Laukaitis, G., Dudonis, J.** Development of SOFC Thin Film Electrolyte Using Electron Beam Evaporation Technique from the Cubic Phase YSZ Powder *Materials Science (Medžiagotyra)* 11 (1) 2005: pp. 9 – 13.
21. **Laukaitis, G., Dudonis, J., Milcius, D.** Deposition of YSZ Thin Film Using Electron Beam Evaporation Technique *Materials Science (Medžiagotyra)* 11 (3) 2005: p. 268.
22. **Laukaitis, G., Dudonis, J., Milcius, D.** YSZ Thin Films Deposited by E-beam Technique *Thin Solid Films* 515 2006: pp. 678 – 682.
23. **Cheary, R. W., Coelho, A. A.** (1996). Programs XFIT and FOURYA, deposited in CCP14 Powder Diffraction Library, Engineering and Physical Sciences Research Council, Daresbury Laboratory, Warrington, England. (<http://www.ccp14.ac.uk/tutorial/xfit-95/xfit.htm>)
24. **Ensinger, W.** Low Energy Ion Assist During Deposition – an Effective Tool for Controlling Thin Film Microstructure *Nuclear Instruments and Methods in Physics Research B* 127/128 1997: pp. 769 – 808.
25. **Wang, H. B., Xia, C. R., Meng, G. Y., Peng, D. K.** Deposition and Characterization of YSZ Thin Films by Aerosol-assisted CVD *Materials Letters* 44 2000: pp. 23 – 28.

Presented at the National Conference "Materials Engineering'2007" (Kaunas, Lithuania, November 16, 2007)

DOI: 10.5755/j02.ms.26353